OPTICAL PROPERTIES OF THE BERING SEA NAVAL ENVIRONMENT JANUARY - FEBRUARY 1960

J. M. Hood, Jr. • Research Report 1150 • 18 December 1962

U. S. NAVY ELECTRONICS LABORATORY, SAN DIEGO, CALIFORNIA • A BUREAU OF SHIPS LABORATORY

THE PROBLEM

Develop optical environmental factors affecting naval surveillance and counter-surveillance requirements and systems. More specifically, obtain polar environmental data (1) for computing and predicting the optical detectability of targets, and (2) for basic geophysical research studies.

RESULTS

Optical and meteorological data were collected during naval exercises in the Bering Sea during the winter of 1960. The data represent the fullest description of sea-level arctic optical conditions presently available. The information can be used for the analysis and prediction of conditions influencing (1) visibility, (2) photographic or photoelectric surveillance, and (3) equipment and personnel operations.

PLANS

The data will be used for continuing studies of sea surface target backgrounds and for studies of remote sensing by optical means of sea and ice conditions. The data will also be coordinated with extensive ground level optical information presently being accumulated at Point Barrow.

ADMINISTRATIVE INFORMATION

The work was done under SF 003 02 03, Task 0533 (NEL N6-4) by members of the Material Sciences Group. The data were gathered during the winter of 1960 and the analysis was completed June 1962. The report was approved for publication 18 December 1962.

CONTENTS

ILLUSTRATIONS

INTRODUCTION

As part of a continuing program of research into the geo-optics of the polar naval environment, a series of investigations was undertaken and data collected during naval exercises in the Bering Sea in the winter of 1960. The purposes of the studies were twofold: (1) to provide information for the computation and prediction of the optical detectability of targets or environmental features of military interest, and (2) to provide data for basic geophysical research studies.

The information recorded, or extracted from recorded data, includes horizontal illuminance, luminance distributions, goniophotometric curves for snow and ice, anomalous atmospheric refraction, photometrically calibrated aerial photographs of the winter Bering Sea surface, and auroral activity. All the measurements were made from stations on or near the ice-breaker USS STATEN ISLAND (AGB 5), in a general area extending from the straits of Unimak Pass to St. Lawrence Island.

For purposes of predicting surveillance conditions and the detectability of targets, the most significant data collected consist of (1) the nearly continuous recording of horizontal (downwelling) illuminance made over the period January 23 through February 23; (2) the series of about 130 photometric photographs made of the sea surface from one of the ship's helicopters; and (3) a series of luminance distributions with the sun at zenith angles between 75° and 96° under both clear and overcast conditions.

SCHEDULE AND DESCRIPTION OF EXPERIMENTS

The following photometric quantities were measured or investigations and observations made:

1. Complete surface weather observations.

2. Horizontal-downwelling illuminance.

3. Luminance distributions.

4. Photometrically calibrated aerial photos of frozen or partially ice-covered sea surface.

5. Observation of sunrise-sunset times for study of refraction anomalies.

6. Goniophotometric properties of snow and ice.

In addition, the complete and accurate ship's track for the experimental period was recorded for later correlation of the recorded data and zone times with true sun and moon positions. Figure 1 summarizes graphically the pattern and frequency of data collection. The shaded bars indicate the presence of some data or observations for that date.

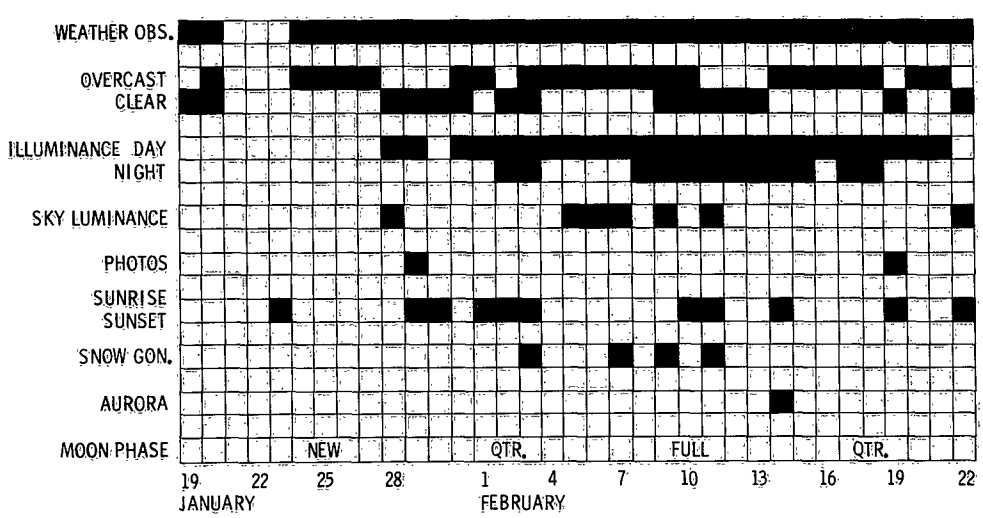

Figure 1. Bering Sea experiment schedule.

The decision to indicate overcast or clear or both was governed to a large extent by conditions prevailing during the data collection portion of the day, exclusive of consideration for the illuminance meter which ran more or less continuously.

Photometric quantities were measured with devices containing photocells corrected by means of filters to the standard photopic spectral response characteristic. An exception was the aerial camera which used an uncorrected plus-*X* emulsion and a visual comparison hand-held photometer which, of course, gave readings referred to the response of a specific human eye.

INSTRUMENTATION

Illuminance Photometer

A photometric system designed and constructed at the Laboratory gave a continuous recording of illuminance. The system consisted of the following elements:

1. Two Lambert-surface (cosine) translucent collecting heads, identical except that the daylight head contained a neutral Wratten filter of about density 3.

2. The detector element, an RCA type 1P21 multiplier phototube with an attached Wratten 106 filter for adjusting the S-4 spectral response to standard photopic response.

3. The heated and thermostatically controlled phototube housing in which temperature was maintained at +25°C. It assured that the precise alignment of the electronic circuitry which had been made with the phototube at room ambient temperature would be preserved under the normally prevailing cold and inclement conditions of the experiment. The heater, in fact, maintained the proper temperature and in addition prevented condensation or deposition of moisture inside the housing or on the optical head.

4. The multiplier-phototube circuit of the constant current circuit type which furnishes an output voltage proportional to the logarithm of the light incident on the photocathode. The dynamic range of the circuit exceeded four decades.

5. The recorder, a Varian G-11 type, having a paper speed of 15 inches per hour with the recording span adjusted to give four decades of illuminance for the 5-inch hundred-unit paper width. The record, easily read to $\frac{1}{2}$ division, afforded a recording precision of 0.02 decade or about 0.05 of the illuminance value recorded. This precision was obtained over the range of more than seven decades spanned by the two optical heads.

The illuminance photometer head was installed at a level about 8 feet above the forward port-side edge of the flight deck. In this position a total of 1350 square degrees of the sky is obstructed by ship's structures and adjacent objects. This total obstruction was determined from the planimetry of a panoramic photo made from the optical head position, and amounts to only 6.5 per cent of the total 20,600 square degrees constituting the solid angle of the entire sky. If the weather is overcast or the sun unobstructed by any of the noted structures, it is estimated that the readings of the instrument will be affected by less than 1 per cent. No readings were transcribed from the recordings corresponding to direct shadowing of the sun by any artificial means.

Luminance Photometer (Small Field)

The luminance photometer with which the luminance distribution measurements were made has as its central feature a very compact, sensitive, yet wide-dynamic-range photometer circuit operated on dry-cell batteries.[1] (See list of references at end of report.) Figure 2 shows this device being used to measure sky luminance. The optical and mechanical portion of the instrument consists of the

long light-baffle tube shown and the small telescope containing the objective lens, field lens, aperture stops (5, 15, 30 minutes of arc), and the RCA 1P21 multiplier phototube. The standard telescope tripod had altitude-azimuth circles from which the telescope position was read. During data collection sessions these angle circles were oriented by first leveling the azimuth circle by successive sightings of the horizon with the scope, setting the elevation circle to 0° and then setting the 0° point of the azimuth circle to the position of the sun or, for overcast conditions, to geographical north.

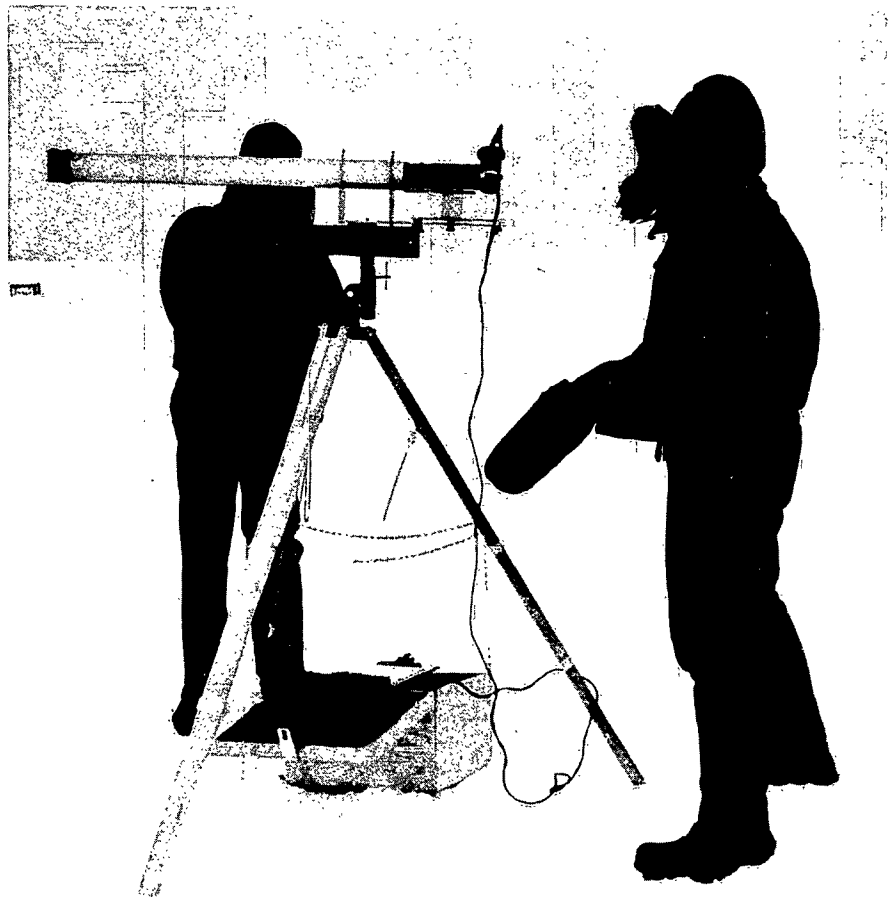

Figure 2. Using photometer to measure sky luminance.

Camera

The photometrically calibrated photographic negatives were made with a standard K-20 hand-held aerial camera. This camera uses $5\frac{1}{4}$-inch 50-exposure roll film. The special calibration technique did not require special handling of the film in processing.[2] The rolls were processed aboard the ship and inspected as the work proceeded.

Other Equipment

In addition to the major devices listed above, some data were collected with a hand-held Luckiesh-Taylor visual photometer.

All absolute photometric calibrations were obtained during the course of measurements with the aid of calibrated light source having a transilluminated plaque of luminance 92.6 foot-lamberts.* This source was checked against National Bureau of Standards photometric standard lamps over an extended period of time both before and after the experiment. No changes in luminance were detected.

METHODS OF ANALYSIS

Geographical Location and Time

Preliminary analysis of the luminance and illuminance data required that a detailed description of the ship's position be prepared. It was elected to divide the geographical

*Calibrated brightness source: Photo Research Corporation, Hollywood, California.

area involved into 30-minute blocks. These blocks are commensurate with maximum possible errors in time measurements, ship position records, and computational precision of the sun and moon position. All data collected in a given block were assigned the latitude and longitude of the center of the block. All time notations on recorder paper, logs, and data sheets were in local standard zone time. These were all later adjusted to (+11) zone time for uniformity in computing.

Illuminance

From calibration records and other qualifying notes, valid illuminance data were blocked out on recorder rolls. These were read at 10-minute time intervals with a special logarithm-scale rule, indexed for absolute calibration and optical head selection (day or night). These raw illuminance data, the date-time, and ship's position were entered on IBM cards from which a set of processed data cards was produced having the date-time, illuminance, log-illuminance, azimuth and zenith angles of the sun's position, azimuth and zenith angles of the moon, and the phase of the moon. The final set of data consisted of about 2000 cards which were then studied by employing a card sorter and a digital plotter.

Luminance

Sky luminance records required special handling to account for the finite length of time required to collect the information. The pattern of telescope motions which resulted in the shortest over-all measurement time consisted of setting the telescope to zenith angle and quickly rotating to each azimuth position. By duplicating the first azimuth reading at the end of the turn and by reading the zenith at the beginning and the end of each complete session, it was possible to determine a time-skew to the luminance pattern.

With the prevailing typically high zenith angles for the sun, the assumption of a simple linear relationship between time and log-luminance enabled the readings, recorded as log [ft-L], to be corrected by application of a simple linear correction factor based primarily on the beginning and ending zenith luminance readings.

These corrected readings were then entered on IBM cards and a computer interpolation analysis made to determine the location of the selected luminance interval values. In the case of the clear skies which covered a relatively large range of luminance, an interval of 0.20 log-cycle was selected. For overcast conditions, which have a much smaller brightness range, the interval selected was 0.05 log-cycle. These intervals represent, respectively, 58 and 12 per cent luminance change per interval.

Since interpolations were calculated between all possible adjacent pairs of readings including diagonals, a grouping of points of a given luminance was frequently obtained and an effective smoothing of the data accomplished in drawing in the isoluminance contours.

Atmospheric Refraction

Values of atmospheric refraction were indirectly determined from a precise recording of the time of sunrise or sunset and the concurrent position of the ship. The equation

$$\sin a = \sin \varphi \sin \delta + \cos \varphi \cos \delta \cos h$$

where a is sun elevation, φ is latitude, δ is solar declination, and h is the solar hour angle, was used to compute the actual position of the sun. In each calculation normal refraction, angle-of-dip for the bridge observing position, and surface temperature-pressure corrections were made. The residue, if any, was called the "anomalous" refraction.

Except for surface temperature and pressure, the above calculations are based on a theoretical model atmosphere giving a refraction of 34 minutes at 90° zenith angle. Data on the vertical atmospheric profile were not available for the exact times or for the ship's positions, but radiosonde data are available routinely from Nome, the nearest weather station. These data were analyzed for optical refraction by the technique of Weisbrod and Anderson.[3] This nomographic method, developed for radio propagation predictions, is remarkably effective and simple in predicting optical refraction as well. One uses the equations as given but neglects the terms involving the electron density which have no consequence at optical wavelengths.

Optical Properties of Snow and Ice

Field instrument limitations imposed certain accuracy restrictions on the collection of goniophotometric curves of the snow and ice surfaces. Ideally one would prefer to have a fresh sample of the surface for photometric examination at all angles of incidence, for various angles of illumination by a narrow collimated source, and with wavelength as a variable as well.

With only the tripod-mounted small-field photometer available, it was necessary to select a very large undisturbed and uniform snow surface for measurement. The point of location of the photometer was approached from a cross-sun direction and measurements of luminance made along a path from horizon-to-horizon aligned with the azimuth of the sun and from horizon-to-nadir in the direction 90° to the azimuth of the sun. This technique is based upon the assumption that all points along the paths had identical optical properties.

Photographic Photometry

Photographs were analyzed by a method described earlier by the author.[2] Basically this method presents several advantages over the standard sensitometric methods normally employed in such photometry. A six-step grey scale is employed and a set of exposures of this scale is made with two to three stop differences in successive exposures. This gives density steps on the several exposures covering a film exposure range of about 500 to 1. When these densities are plotted as ordinates against a log-reflectance scale, a set of vertically separated curves results. An empirically determined factor of the abscissa values is introduced to all but one of the curves by sliding the curves horizontally until a best smooth fit is obtained. The resulting curve is the luminance transfer function for the film-lens-camera body combination and, if care is used, accounts for lens and camera body scattering not normally accounted for in ordinary sensitometry. The advantages are that special processing equipment, sensitometric facilities, or other devices except for the painted grey scale are not required in the field. Pictures can be processed immediately and inspected before the opportunity for additional pictures has passed. And, of course, the total contrast transfer function for system is obtained directly and simply.

RESULTS

Illuminance - Day

The illuminance data must be dealt with in two parts, for day and for night. About 75 per cent of the illuminance measurements show an overriding influence of the sun's presence and are considered daytime data.

Figure 3 is a comprehensive plot of all these sun-influenced illuminance data. Shown superimposed is

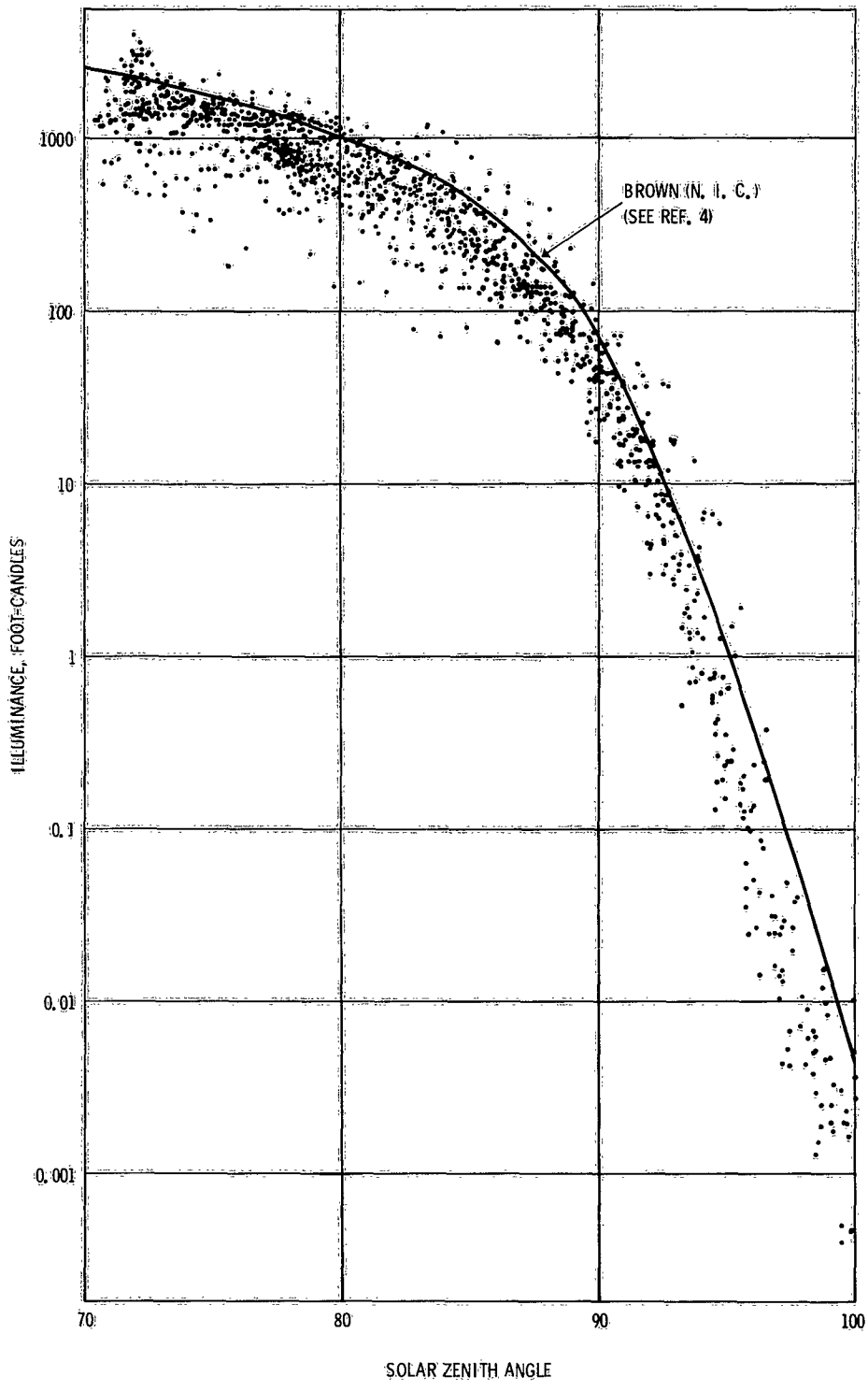

Figure 3. Solar illuminance.

Brown's average clear day illumination curve for these sun-zenith angles.[4] If the weather pattern is noted from figure 1 and the samples of daily curves shown in figures 27 and 28 (pages 30 and 31) are noted for their generally smooth shape, the obvious conclusion is that the variation in illuminance at a given sun-zenith position is a function of cloud cover. The upper bound of the data should then represent illumination for a clear winter environment and the lower bound that for totally overcast conditions.

Night Illuminance and Aurora

Figure 4 shows the illuminance curves produced from four nights covering a 5-day period near the time of the full moon. Practically no data were collected at times of no moon influence, and the sensitivity limit of the equipment itself was imposed at about 10^{-4} ft-candles. For each of the curves plotted the moon phase is noted. The difference in the right ascensions of the sun and moon is taken as the definition of phase in this study. For each night are noted the cloud cover and weather condition.

Two evident features of these curves are:

1. Excessive variability of the data points for 2/13-14 and 2/14-15.

2. The decidedly anomalous values shown for the evening of 2/14 and the similar but smaller indication shown for the mornings of 2/14 and 2/15.

Unfortunately the variability characterized by the data of 2/10-12 is a limitation caused by precision limits of the recorder - photometer system and not by any real variation in the illuminance. That shown for 2/13-15, however, can certainly be attributed to the broken overcast conditions in the first instance and the snow storm in the second case.

During the experiments, the investigators and the men of the bridge watch kept alert for auroral occurrences for direct correlation with photometer records. None were observed during the period of data collection. Such observations were possible only during clear conditions. Extracting the occurrence of aurora from the records themselves seemed a distinct possibility, since the prediction of night illuminance values is relatively straightforward and simple. The anomalous, high values noted above are the only suspect data found from a careful search of all the records.

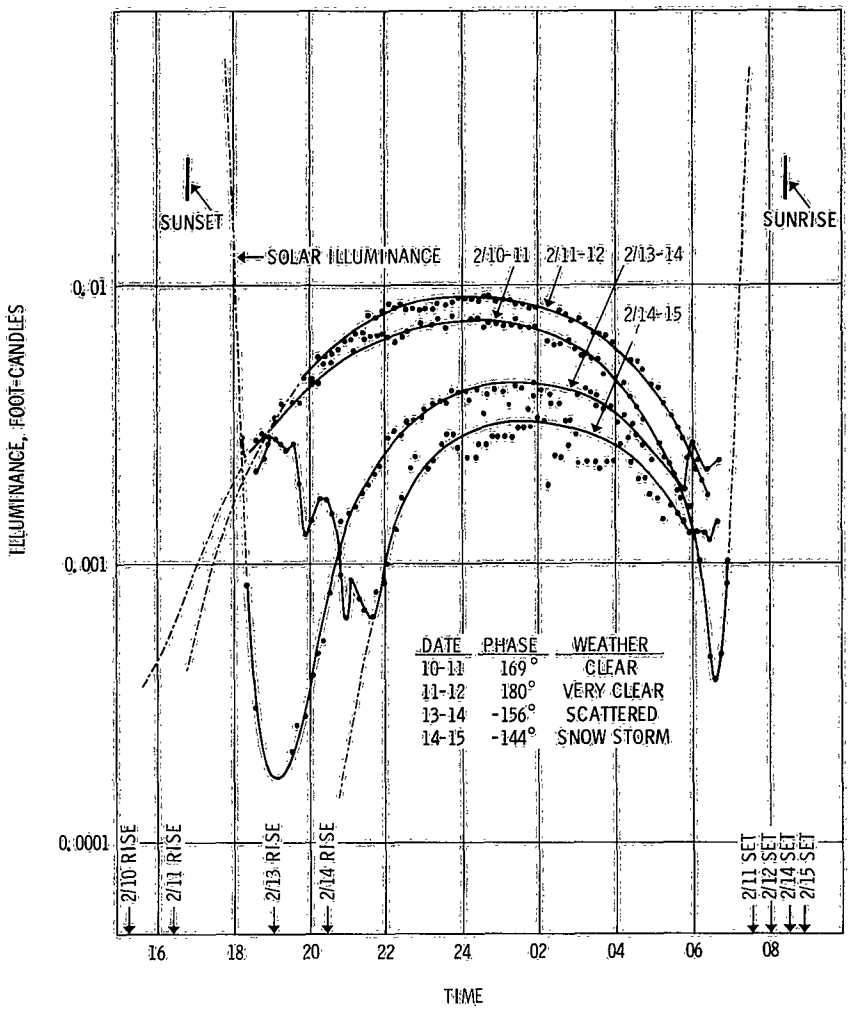

Figure 4. Moon influenced illuminance.

One can conclude that at least on the evening of 2/14 there was an occurrence which increased the illuminance by a factor of about ten over the normal condition or to about the amount of light of a full moon high in the sky. It seems reasonable that this increase could only have been caused by an aurora.

Figure 4 also indicates as dashed curves the average twilight solar effect and possible extrapolations of three of the moonlight curves based on indications shown by the curve of 2/13-14.

Luminance Distributions

Table 1 lists every occasion of luminance distribution measurement. These measurements cover the available conditions of cloud cover from clear to heavy overcast and a sample of sun zenith angles to the low level limits of the photometer. Concurrently noted in the table are values of illuminance read from the records of the illuminance photometer at the mid-session time for each sky measurement.

It should be noted that the values given on the isoluminance lines in figures 5 through 25 are the logarithms of luminance measured in foot-lamberts. The intervals selected for clear skies and for overcast skys are different, being 0.2 unit for the former and 0.05 for the latter. On sky No. 11 it was recorded that a "white-out" condition seemed to exist and yet the measurements showed a relatively highly structured brightness pattern. In all cases the air was relatively clear and good horizontal visibility prevailed.

TABLE 1. SKY LUMINANCE DISTRIBUTIONS NOTING GENERAL WEATHER CONDITIONS, DATE-TIMES, AND SIMULTANEOUSLY RECORDED ILLUMINANCES. BERING SEA, WINTER 1960.

No.	Date	Time	Sun Zenith(°)	Illuminance (ft-c.)	Weather
1	28 Jan	1211	81.2	1100	Clear
2	5 Feb	1045	81.5	550	Watery sun
3	6 Feb	0829	91.5	11	Overcast
4	6 Feb	0917	88.3	160	Overcast
5	6 Feb	1203	78.5	890	Overcast
6	6 Feb	1330	79.0	715	Overcast
7	7 Feb	0943	84.8	340	Overcast
8	7 Feb	1108	79.5	720	Overcast
9	7 Feb	1426	80.9	926	Clear
10	9 Feb	1425	80.2	520	Clear
11	9 Feb	1643	91.1	24	Thin overcast
12	9 Feb	1657	92.5	6.4	Overcast
13	11 Feb	1226	75.5	1710	Clear
14	11 Feb	1650	90.7	16	Clear
15	11 Feb	1705	92.4	3.7	Clear
16	11 Feb	1719	94.0	0.49	Clear
17	11 Feb	1734	95.5	0.055	Clear
18	22 Feb	0904	90.6	346	Clear
19	22 Feb	0916	89.2	462	Clear
20	22 Feb	0936	87.1	830	Clear
21	22 Feb	0956	85.0	1260	Clear

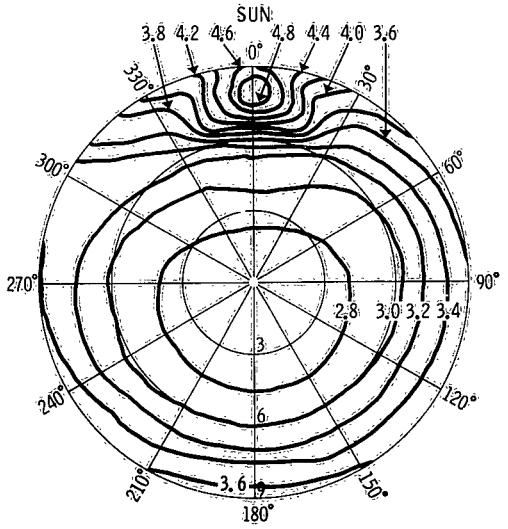

Figure 5. Isoluminance diagram, sky no. 1, 62° 12' N, 174° 58.8' W, snow over sea ice, clear, wind 20 knots, sun elevation +8.8°.

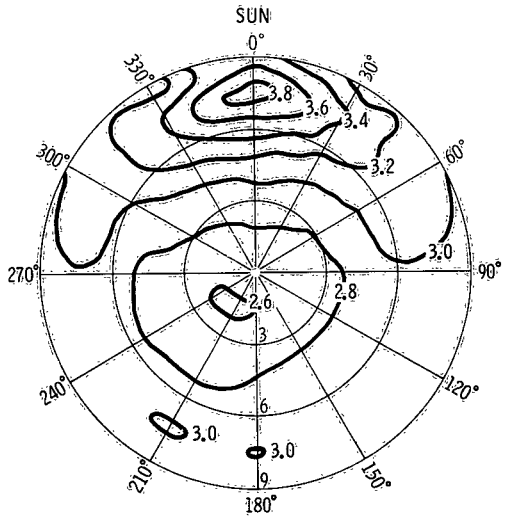

Figure 6. Isoluminance diagram, sky no. 2, 62° 33.2' N, 169° 06' W, snow covered ice, watery sun, wind 30 knots, sun elevation +8.5°.

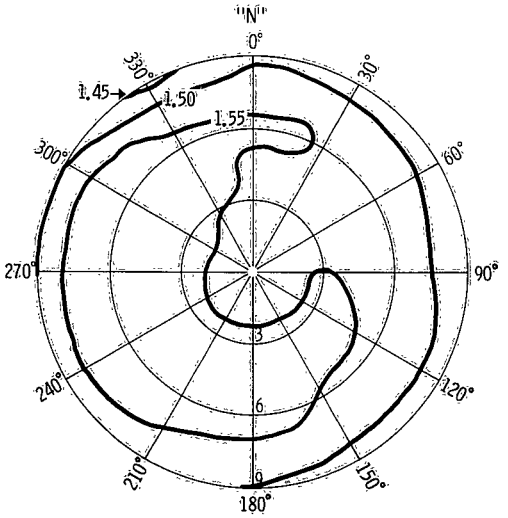

Figure 7. Isoluminance diagram, sky no. 3, 62° 12' N, 169° 42' W, snow covered ice, overcast, sun elevation -1.55°.

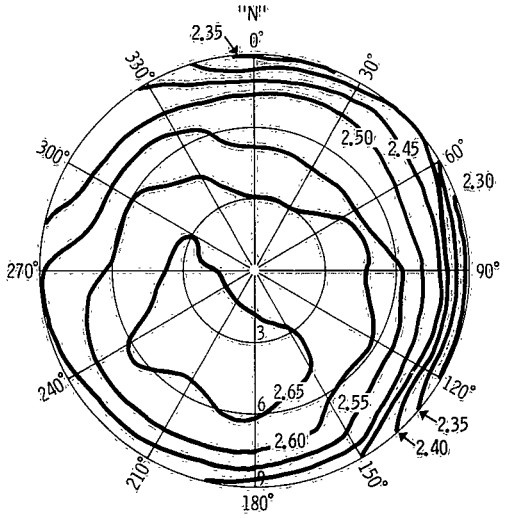

Figure 8. Isoluminance diagram, sky no. 4, 62° 12' N, 169° 42' W, snow covered ice, overcast, wind 22 knots, +8°F, sun elevation +1.66°.

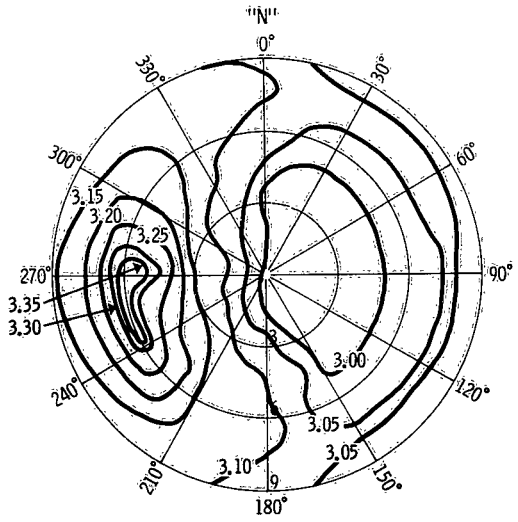

Figure 9. Isoluminance diagram, sky no. 5, 62° 12' N, 169° 42' W, snow covered ice, overcast, sun elevation +11.5°.

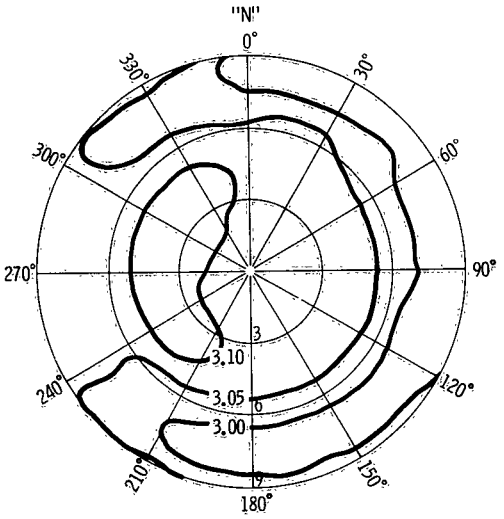

Figure 10. Isoluminance diagram, sky no. 6, 62° 12' N, 169° 42' W, snow covered ice, solid overcast, no structure, sun elevation +11°.

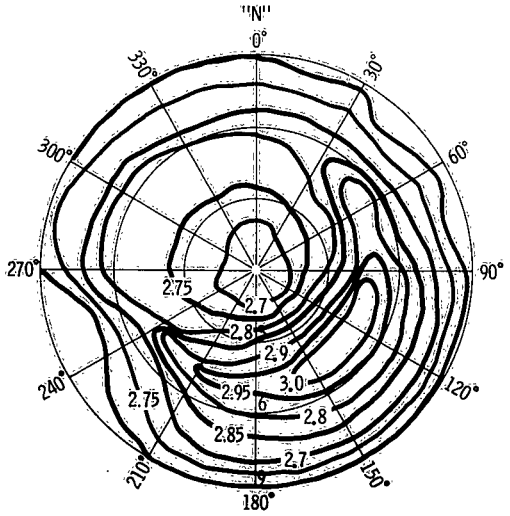

Figure 11. Isoluminance diagram, sky no. 7, 62° 14' N, 169° 41' W, fresh snow covered ice, complete overcast, sun elevation +5.2°.

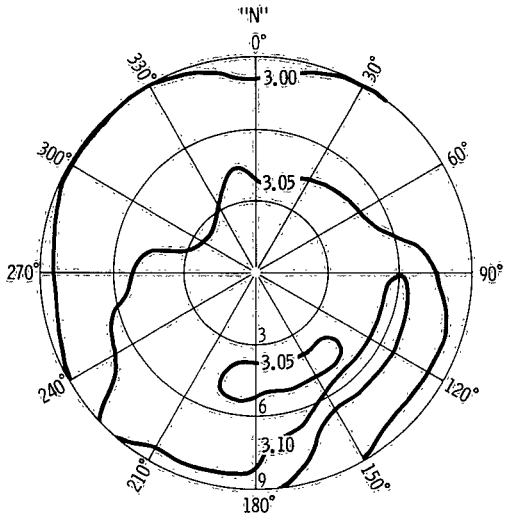

Figure 12. Isoluminance diagram, sky no. 8, 62° 05.5'N, 169° 99' W, fresh snow on ice, solid overcast, visibility good, sun elevation +10.5°.

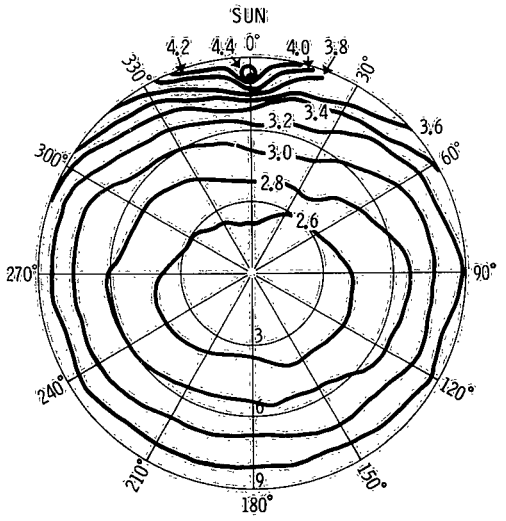

Figure 13. Isoluminance diagram, sky no. 9, 62° 05.5' N, 169° 39' W, fresh snow covered ice, clear, sun elevation +9.1°.

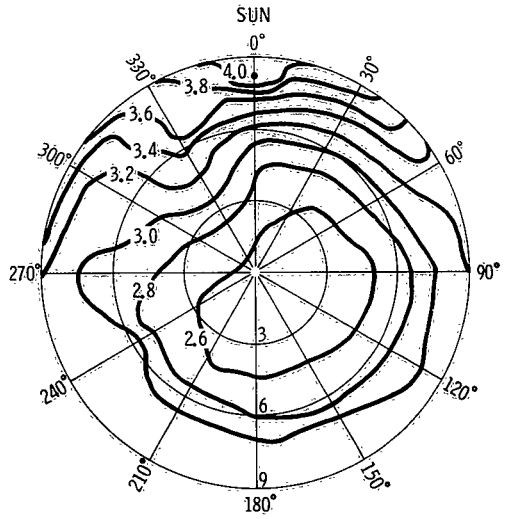

Figure 14. Isoluminance diagram, sky no. 10, 61° 41.5' N, 169° 45' W, wind driven snow over ice, clear, scattered cirrus clouds, sun elevation +9.8°.

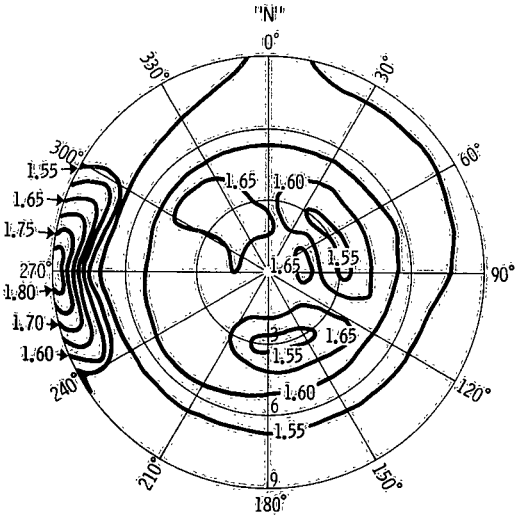

Figure 15. Isoluminance diagram, sky no. 11, 61° 44' N, 169° 45.2' W, snow covered ice, thin overcast, almost white-out, sun elevation -1.1°.

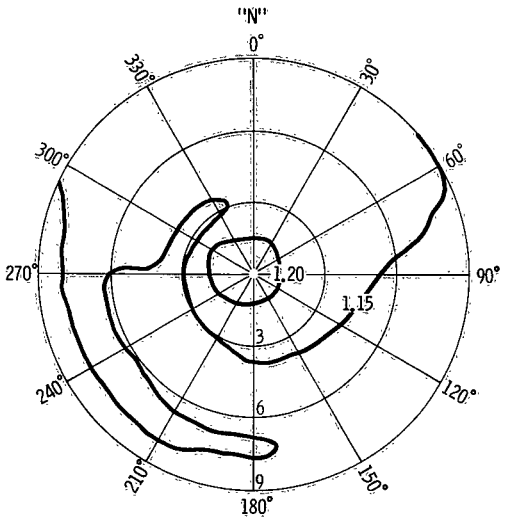

Figure 16. Isoluminance diagram, sky no. 12, 61° 44.5' N, 169° 45.2' W, snow covered ice, overcast, sun elevation -2.5°.

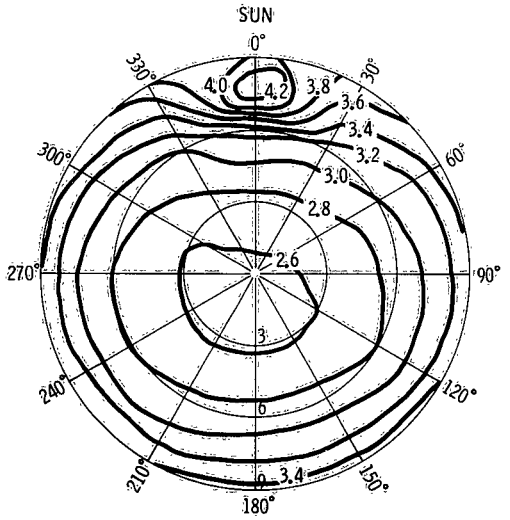

Figure 17. Isoluminance diagram, sky no. 13, 61° 07' N, 169° 47.5' W, snow covered ice, clear, few clouds on horizon, sun elevation +14.5°.

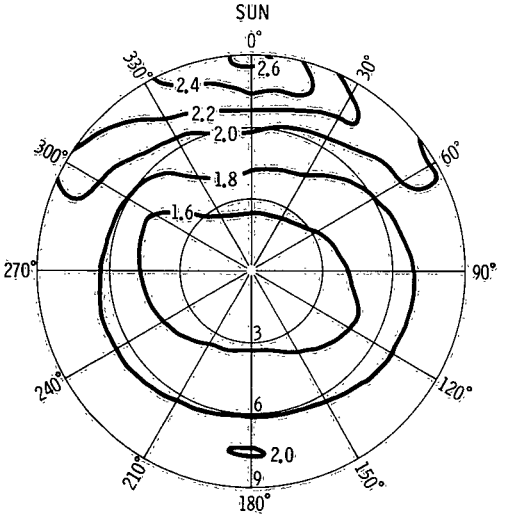

Figure 18. Isoluminance diagram, sky no. 14, 61° 05' N, 169° 56.1' W, snow covered ice, clear, sun elevation -0.7°.

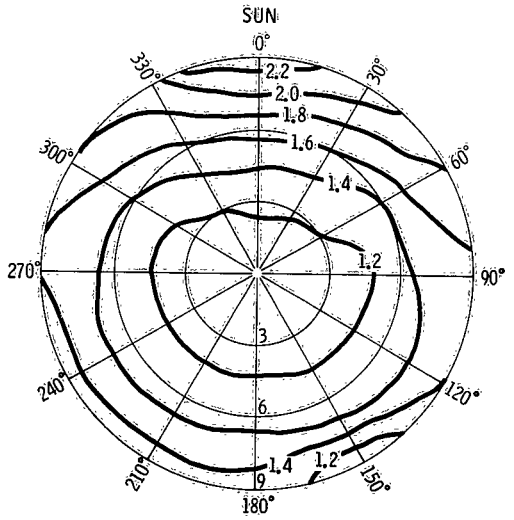

Figure 19. Isoluminance diagram, sky no. 15, 61° 05' N, 169° 56.1' W, snow covered ice, clear, sun elevation -2.4°.

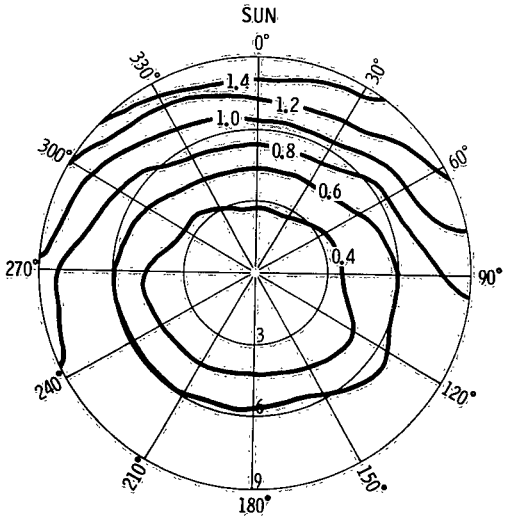

Figure 20. Isoluminance diagram, sky no. 16, 61° 05' N, 169° 56.1' W, snow covered ice, clear, sun elevation -4°.

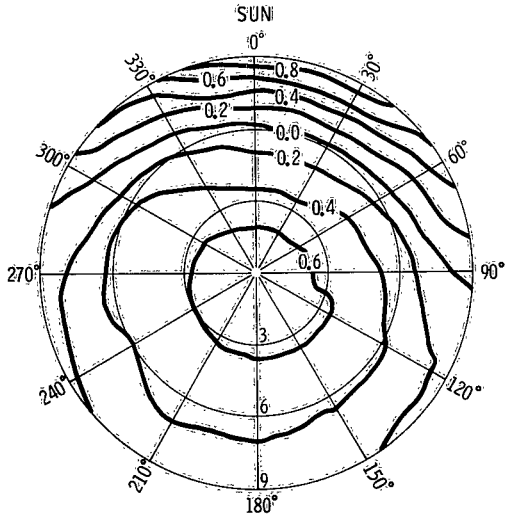

Figure 21. Isoluminance diagram, sky no. 17, 62° 05' N, 169° 56.1' W, snow covered ice, clear, sun elevation -5.5°.

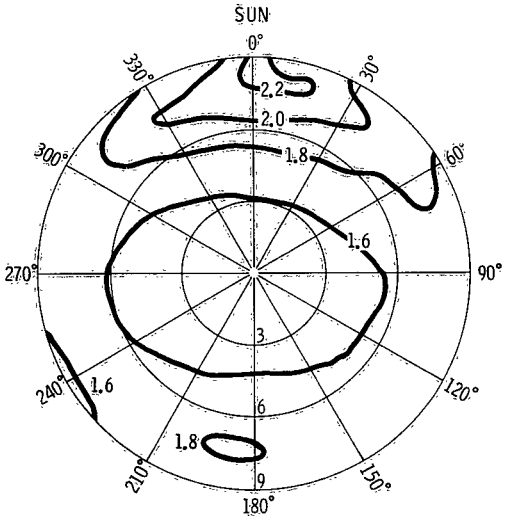

Figure 22. Isoluminance diagram, sky no. 18, 61° 21.7' N, 174° 02.3' W, snow covered ice, clear, some clouds on horizon, sun elevation -0.6°.

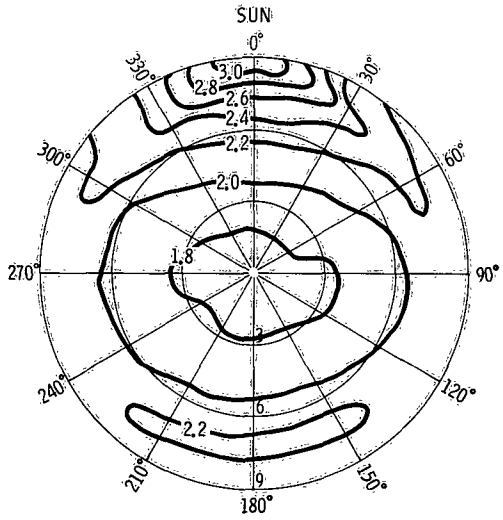

Figure 23. Isoluminance diagram, sky no. 19, 61° 21.7' N, 174° 02.3' W, snow covered ice, clear, sun elevation +0.8°.

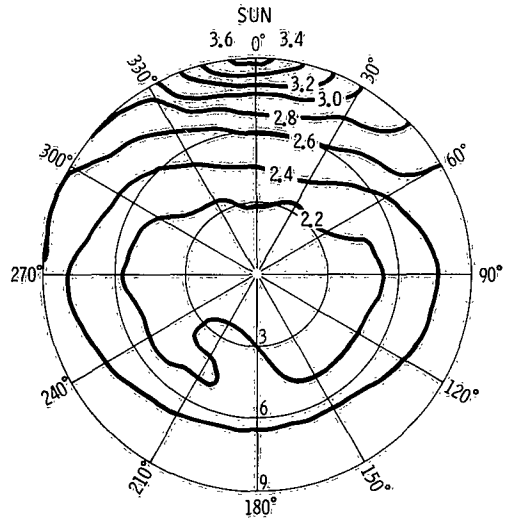

Figure 24. Isoluminance diagram, sky no. 20, 61° 21.7' N, 174° 02.3' W, snow covered ice, clear, some clouds along horizon, sun elevation +2.9°.

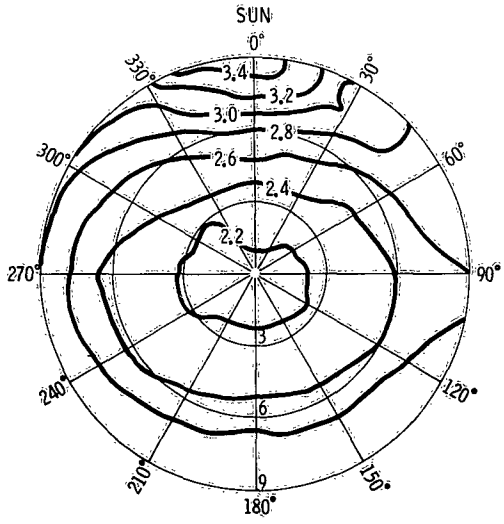

Figure 25. Isoluminance diagram, sky no. 21, 61° 21.7' N, 174° 02.3' W, snow covered ice, clear, some clouds along horizon, sun elevation +5.0°.

Atmospheric Refraction

The measurements of atmospheric refraction which were made by recording exact times of sunset and sunrise on several occasions are presented in table 2. Figure 26 shows schematically the relationship of the various quantities listed in the table and illustrates the method by which the refractions were determined from the calculated astronomical position of the center of the solar disc for the time of observation.

TABLE 2. TOTAL ATMOSPHERIC OPTICAL REFRACTION.*

Date	(a)	(b)	(c)†	(d)	(e)
29 Jan (S)‡	-105.0	-6.9	-43.2	84.1	43.7
30 Jan (S)	-83.8	-6.9	-20.8	61.7	71.3
1 Feb (S)	-59.0	-4.6	+1.7	36.9	85.9
2 Feb (R)	-92.7	-4.6	-32.0	70.6	132.5
2 Feb (S)	-66.3	-5.7	-4.5	44.2	86.5
3 Feb (S)	-63.6	-6.9	-0.6	41.5	32.9
10 Feb (S)	-66.4	-6.9	-3.4	44.3	41.2
11 Feb (R)	-79.5	-6.9	-16.5	57.4	40.8
11 Feb (S)	-69.5	-6.9	-6.5	47.4	42.7
14 Feb (R)	-71.2	-5.7	-9.4	49.1	101.68
19 Feb (R)	-93.2	-4.6	-32.3	70.9	37.5
22 Feb (R)	-89.0	-2.8	-10.1	46.9	35.0

(a) Observed solar elevation calculated from time and ship's position.

(b) Surface temperature-pressure correction term added to observed elevation to obtain actual elevation.

(c) Anomalous refraction obtained by subtracting [(b) + (-6.1 angle of dip) + (-16.0 min. for solar semidiameter) + (-34.0 min. for standard atmosphere)] from (a).

(d) Observed refraction = negative of [-34.0 for standard atmosphere + (b) + (c)].

(e) Radiosonde computed refraction.

* All values in minutes of arc.

† Negative sign indicates additional, unaccounted for, refraction.

‡ (S) Sunset, (R) Sunrise.

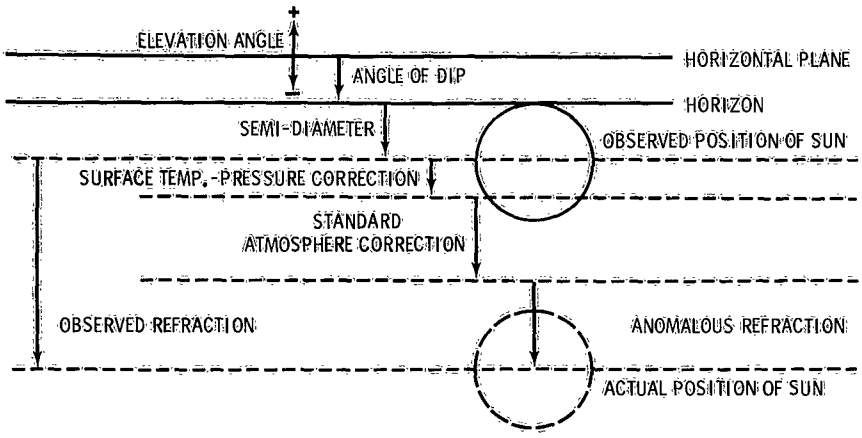

Figure 26. Schematic showing relationship of quantities in table 2.

The question of unpredictable optical refractions at very low angular altitudes has long been of interest in the construction or correction of astronomical navigation tables. The variability of these refractions and the lack of success in predicting them from tables has been observed by Smiley[5] and others to be greatly enhanced in the arctic regions. Fletcher[6] treated this problem with considerable thoroughness and concluded that present tables should stand, until an improved model of the atmosphere is obtained accounting for detailed temperature structure and providing a simple means of including proper corrections in navigation tables. Strand[7] reached a similar conclusion from his careful observations at the Dearborn Observatory. Since the inception of the discussions that have revolved around this point, there has been the suggestion that aside from the implied navigational interest there may be significant effects of this added refraction on horizontal illuminance when the sun is near the horizon. In verbal discussions at the 29th[8] meeting of the NRC - Armed Forces Vision Committee, an opinion was presented that these can amount to as much as a degree or a sizeable fraction thereof and that the level of illumination near the pole can consequently vary substantially from the predicted values for long periods of time.

The two primary objectives of these observations were to determine if such refractions do occur with any considerable frequency and to study the effect of such occurrences on the horizontal illuminance.

The observations were divided into two groups roughly representative of large refraction and little or no refraction. The illumination data for each of the observation times were then plotted according to this division as a function of astronomical sun position. These plots are shown in figures 27 and 28. At first glance it seemed that the large amount of scatter apparent in the figure 27 data could be related to the anomalous refraction. The data were replotted with a shift in the location of the illuminance curve by an amount equal to the observed refraction. This procedure gave no statistical indication of any relationship between the illuminance and the refraction nor did it significantly reduce the scatter in the measured illuminance data.

It seemed desirable also to try and calculate as exactly as possible the actual refraction for the times of observation. The most nearly appropriate data that can be found are the radiosonde data of Nome, Alaska, published by the U. S. Weather Bureau.[9] This information is available for only two times each day, and the location is sufficiently different that very little correlation at the lowest elevations could be expected. The method of Weisbrod and Anderson[3] was used to compute actual optical refractions of the entire atmosphere for the case of sun elevation equal to zero degree. These computations are listed in the last column of table 2. Acceptance of the hypothesis of zero correlation at the .99 confidence level between the observed and calculated values shows that the prediction technique is not adequate to explain the observed refractions. Since the refraction cannot be predicted from radiosonde nor any observed relationship to illumination be demonstrated, it is reasonable to conclude that anomalous refraction is a purely local phenomenon. Typically many unusual and often spectacular optical phenomena occur in the arctic regions. Excepting the aurora, these nearly all

originate in the lowest layers of the atmosphere and often involve temperature inversions in the lowest few meters. Anomalous refraction for either large or small zenith angles certainly can occur at these lowest levels and can interfere with navigation, but it cannot to any measurable extent affect illumination of the surface. Illuminance of

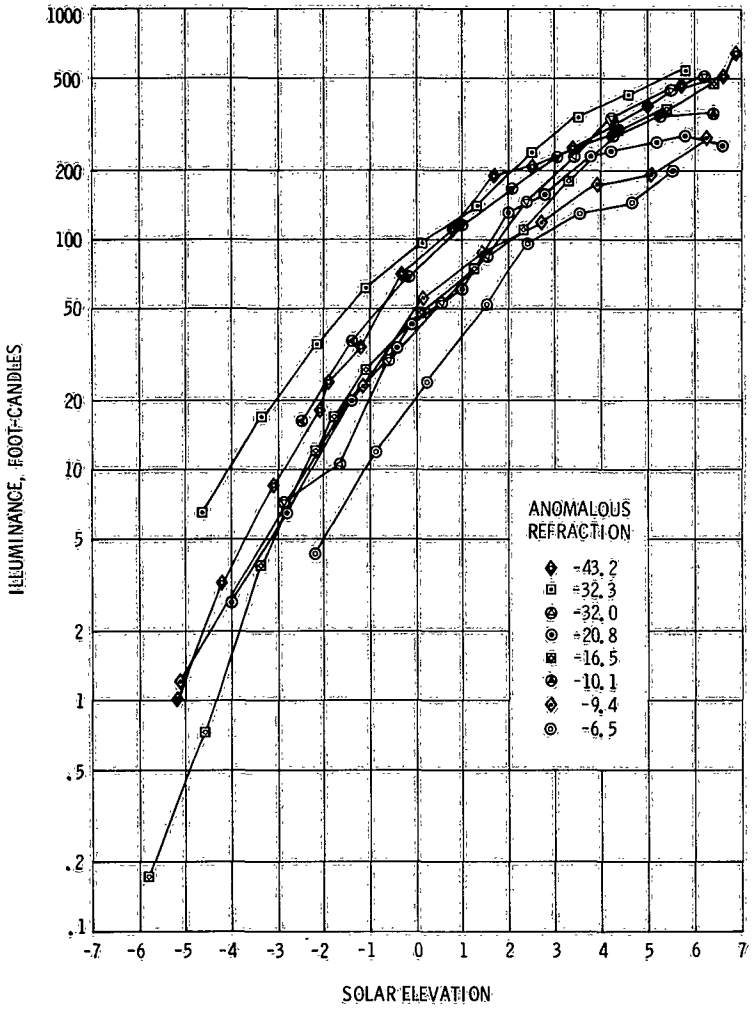

Figure 27. Horizontal illuminance versus solar elevation for days of high refraction.

the horizontal plane at times near sunset or sunrise arises almost entirely from sky light and, of course, this radiation originates from scattering from the entire atmosphere which in the bulk is illuminated directly by sunlight not passing through the more highly and anomalously refracting low layers.

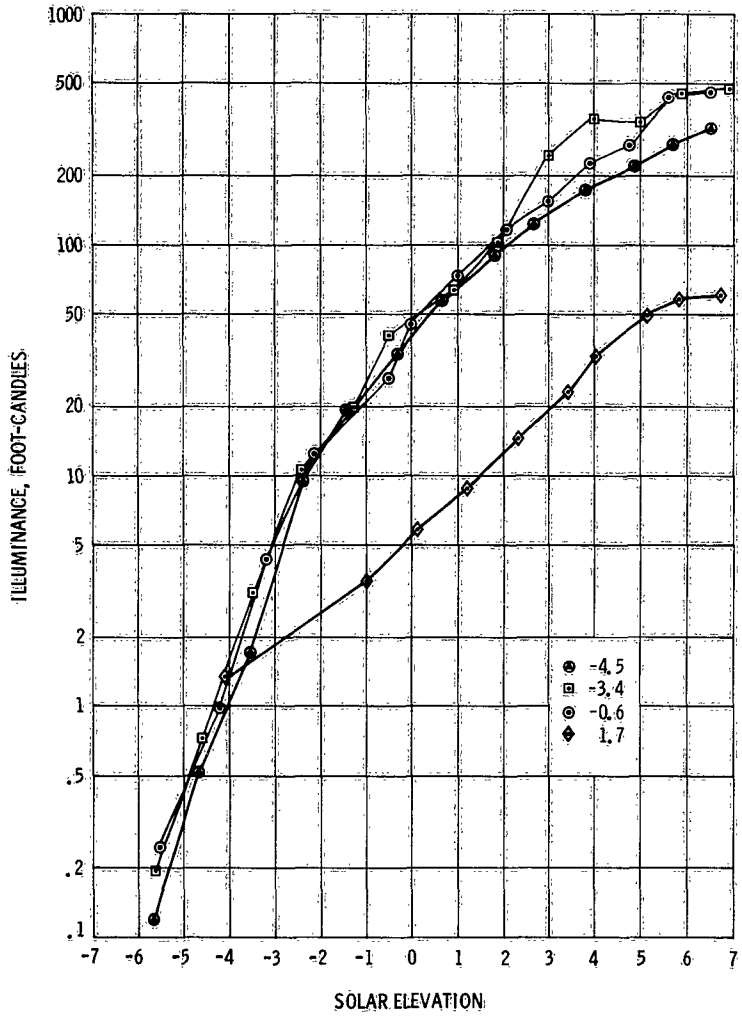

Figure 28. Horizontal illuminance versus solar elevation for days of low refraction.

Goniophotometric Functions for Snow

Figures 29 through 31 present the data collected on the goniophotometric functions for snow. This information is incomplete and reveals only what might have been logically expected from a simple qualitative description of the snow

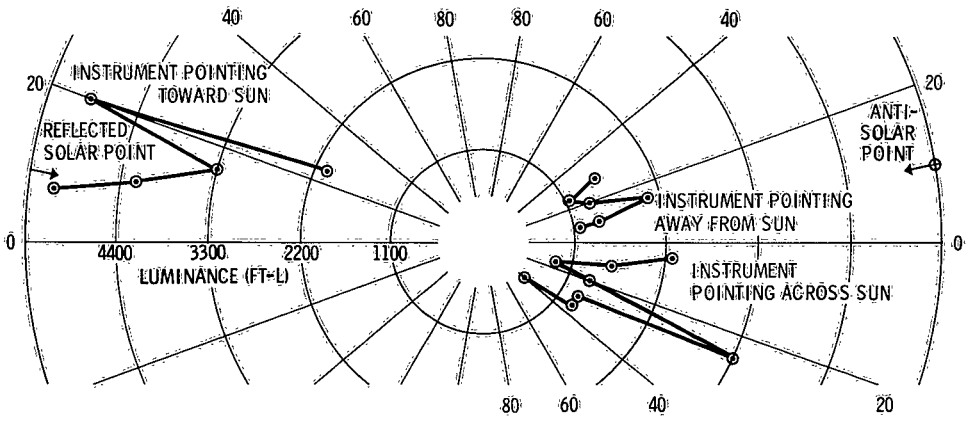

Figure 29. Snow goniophotometry, 7 February 1960, 62° 05.5' N, 169° 39' W, new snow on ice, sun elevation 9.1°, clear.

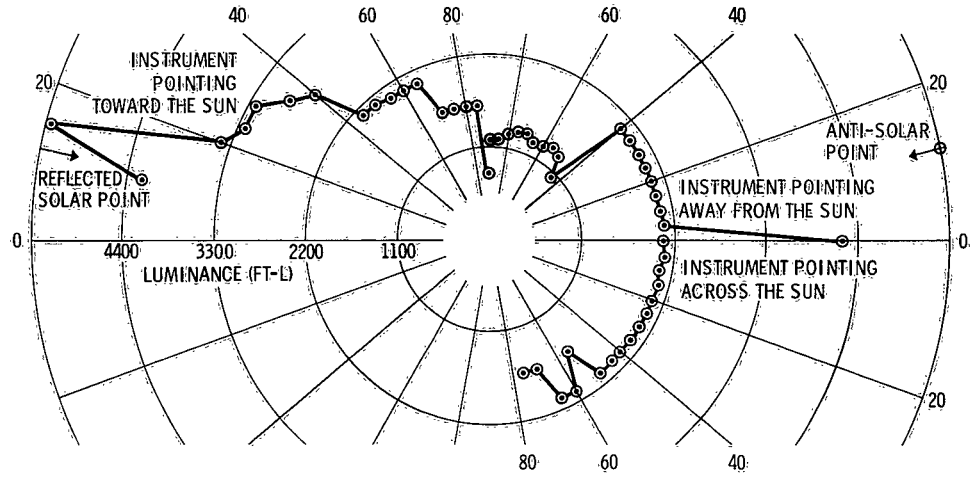

Figure 30. Snow goniophotometry, 9 February 1960, 61° 46.5' N, 169° 45' W, surface-wind crusted snow, sun elevation 11.5°, 20 per cent cirrus.

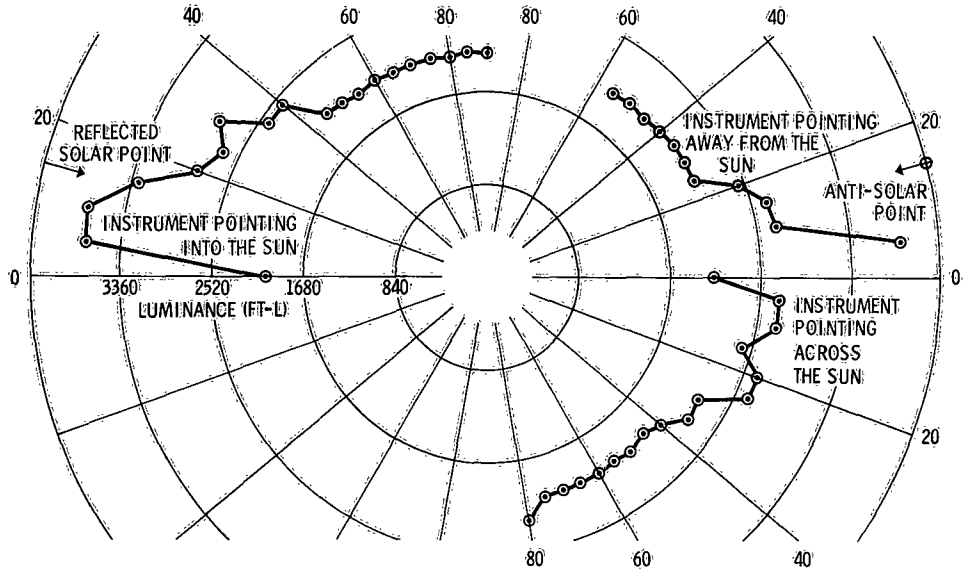

Figure 31. Snow goniophotometry, 11 February 1960, 61° 07' N, 160° 47.5' W, surface-wind packed hard snow, sun elevation 14.5°, clear.

surfaces measured. The hard wind-packed snow surfaces exhibit the expected specular property at large angles of incidence near the reflected solar point. Future measurements of these functions should include smaller incident angles of illumination and, indeed, a wider range of incident angles for the illuminating source. It would then be possible to characterize fully the variation in optical properties expected as a function of the variation in the physical structure of the surface. Middleton and Mungall's study of snow surfaces in Canada has to date provided the only reliable means for predicting the appearance of various types of snow surfaces as a function of angle of view and angle of illumination.[10]

Two factors which have confounded the measurements presented here are: (1) the ergodic assumption that the geometrical properties of the surface scanned by the photometer are invariant with position along the line of scan is probably incorrect, and (2) the level and conditions of illumination are not sensibly invariant during the time required for recording the measurements.

Photographs

Figures 32 through 36 are examples of the 134 calibrated photographs obtained. Relative brightness relationships are available in each of the photographs from simple microdensitometry of the negatives. Studies of the goniophotometric functions for snow and ice surfaces, floe size distributions, and pressure ridge formation and its influence

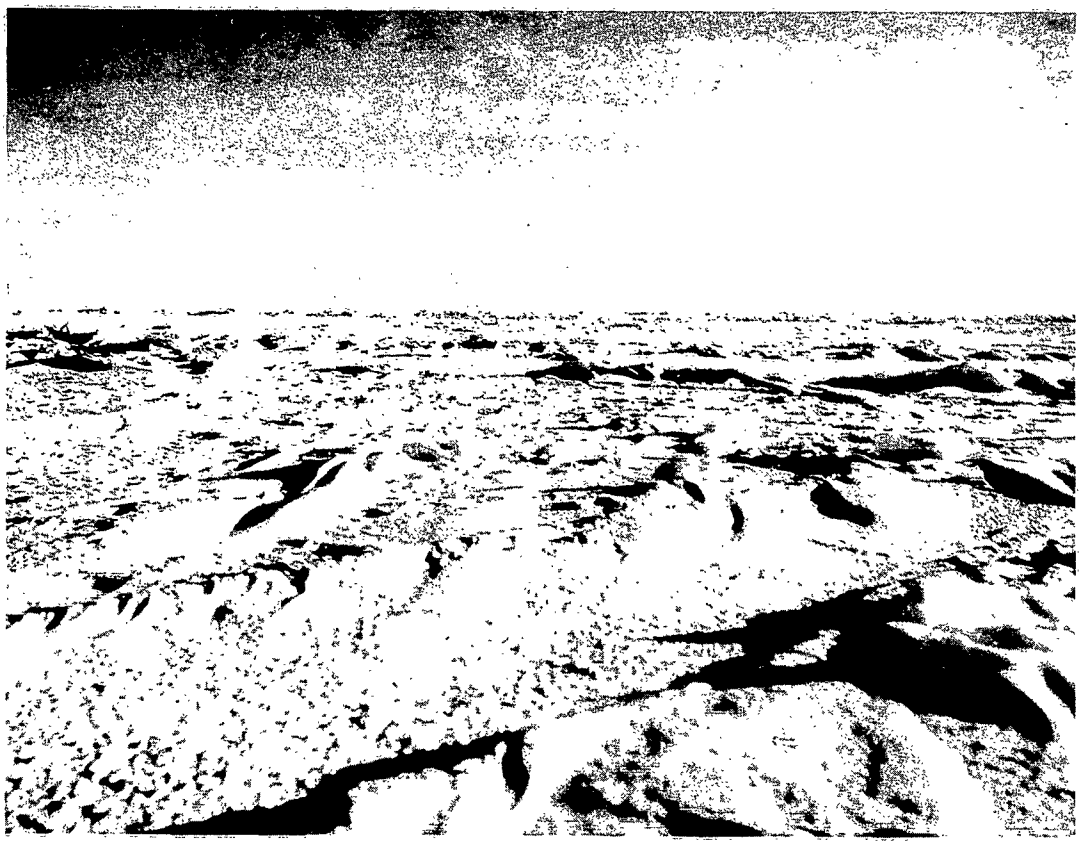

Figure 32. Photograph of sea-ice surface, showing effect of geometric structure of appearance. Grazing angle, large scale, close view.

on optical parameters using these pictures and other data are still underway and will be reported at a later date. Figures 32 and 33 are examples of the same surface at very different scale and angle of view. The changing appearance and integrated luminance of flat areas and of shadowing by ridges and the nature of the small-scale detail effects are apparent in comparing these two examples.

Figure 33. Photograph of sea-ice surface, showing effect of geometric structure on appearance. High angle, small scale, distant view.

Figure 34 is an example of the loose pack near the edge of the ice pack. The characteristic polygonal shape of floes and the distribution of sizes are apparent. Figure 35 depicts a typical lead and also includes good examples of darker new ice forming in the open water as well as relatively snow-free refrozen leads. The various conditions and past history of sea ice can be easily interpreted visually from pictures such as these, but it is the aim of the further studies mentioned above to develop more precise means of interpretation.

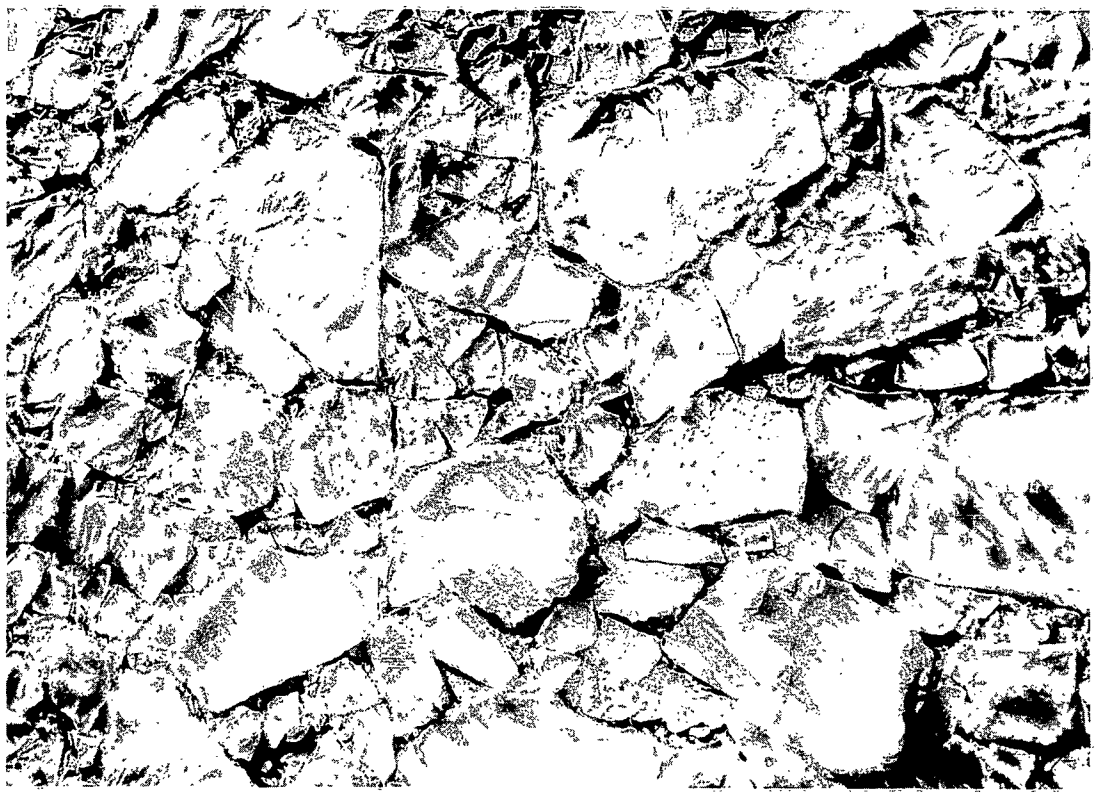

Figure 34. Characteristic floe forms of loose ice pack.

The importance of micro and macro geometrical surface profile on the goniophotometric reflectance functions is graphically shown by figure 36. The "oily" appearance of the surface of the sea in this photograph has been described as imparting a model or miniature effect to the scene. This description is easily understandable on the basis of the physical state of the water in the vicinity of the ship. The water here at the edge of the pack contained

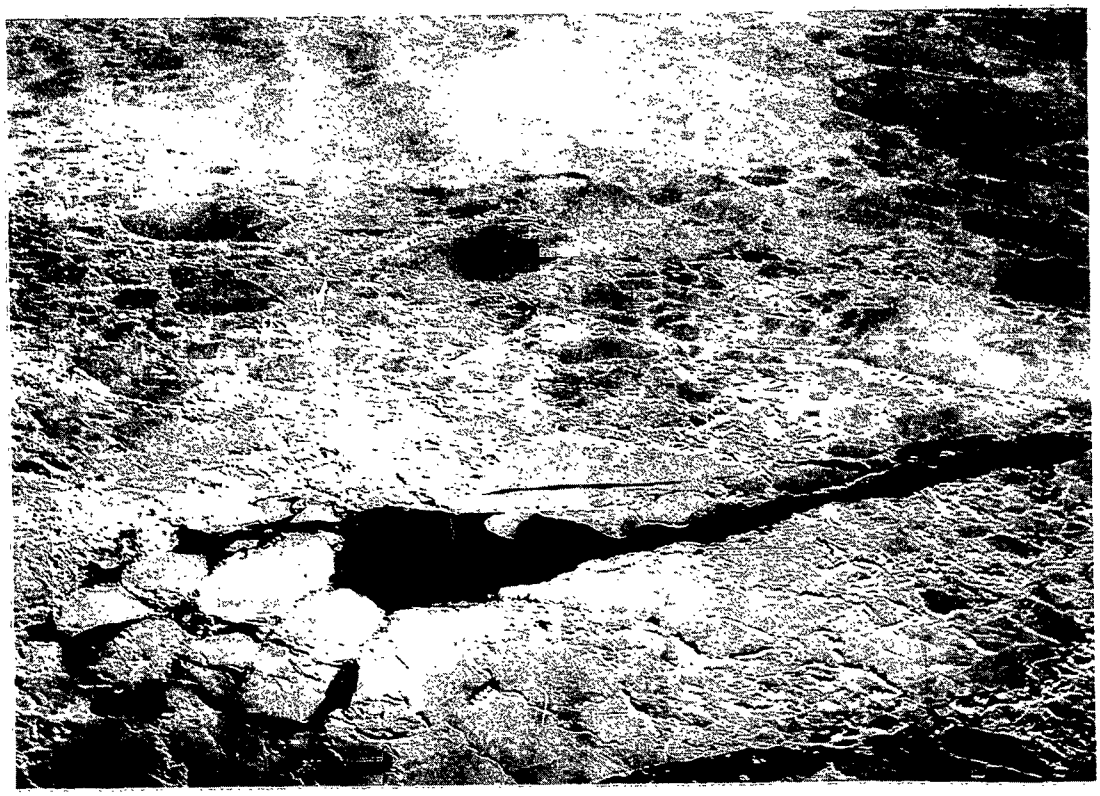

Figure 35. A typical lead.

Figure 36. Effect of fine mushy ice on appearance of sea surface.

a floating layer of fine mushy ice that effectively damps out all the small wavelets which are ubiquitous in normal seas and which profoundly affect the reflectance of light from localized sources. These impart the normal appearance to the sea.

It is not possible, of course, to completely determine a goniophotometric reflectance profile from a single point of view; but many pictures, carefully calibrated, and taken at a variety of angles of the same general area will produce in future studies such profiles. In conjunction with these pictures, photoelectric equipment now being designed and constructed will provide statistical, spatial power spectra, and polarization data.

CONCLUSIONS AND PLANS

The information given represents the fullest description of sea-level optical conditions presently available on the arctic winter naval environment. It provides limited basic data required to predict conditions influencing visibility, photographic or photoelectric surveillance of an important naval operating area, and light and illumination intensity affecting arctic personnel and equipment operations.

In particular, the photographs obtained will be used in continuing studies of sea surface target backgrounds and in studies of remote sensing by optical means of sea and ice conditions. Future studies will attempt to relate the signals and pictures obtained from weather and other satellites to these precise photometric descriptions.

The luminance distributions and the illuminance records in conjunction with the photometric photographs of the surface will permit calculated predictions to be obtained of the photoelectric, photographic, and visual detectability of surface objects and targets. These data can also serve as inputs in laboratory simulation experiments often required to analyze complicated detection and recognition problems involving targets of complex form and pattern.

These data are supplementary to a program of optical studies underway at Point Barrow, Alaska. In particular, the Barrow data do not include the photography although they do include a much more comprehensive ground level study than could be carried out aboard ship. By later comparison with luminance distribution and illuminances obtained aboard USS STATEN ISLAND, it is hoped that the more extensive Barrow data can be related to the sea-ice surface studies. Additional sea, ice, terrain, and cloud studies are being initiated to extend and develop the methods of remote optical sensing of the physical properties of natural surfaces and backgrounds.

A significant point revealed by the sunset-sunrise observations is that the conjectured prolongation of twilight illuminance by the so-called arctic anomalous refraction seems not to be tenable in light of indications of the data on illuminance obtained and the measurements of refraction.

REFERENCES

1. Akin, R. H., "A Portable, Transistorized, Photomultiplier Photometer (Abstract)," Optical Society of America. Journal, v. 48, p. 283, April 1958

2. Hood, J. M., Jr., "Environmental Photometry in the Antarctic," Journal of Geophysical Research, v. 65, p. 1527-1534, May 1960

3. Weisbrod, S. and Anderson, L. J., "Simple Methods for Computing Tropospheric and Ionospheric Refractive Effects on Radio Waves," Institute of Radio Engineers. Proceedings, v. 47, p. 1770-1777, October 1959

4. Bureau of Ships. Code 374 Report 374-1, Natural Illumination Charts, [by D. R. E. Brown], September 1952

5. Smiley, C. H., "Atmospheric Refraction at Low Angular Altitudes in the Polar Regions," Navigation, v. 3, p. 81-84, March 1952

6. Fletcher, A., "Astronomical Refraction at Low Altitudes in Marine Navigation," Institute of Navigation, London. Journal, v. 5, p. 307-330, October 1952

7. Arctic, Desert, Tropic Information Center Publication A-102, Investigation of Atmospheric Refraction at Low Altitudes, by K. G. Strand, February 1953

8. Armed Forces - NRC Vision Committee, Minutes and Proceedings of the Twenty-Ninth Meeting of the Armed Forces - NRC Vision Committee; November 16-17, 1951, p. 20-22, 16-17 November 1951

9. Weather Bureau, Synoptic Weather Maps, Daily Series; Part II: Northern Hemisphere Sea Level and Upper Air Data Tabulations, January 1952 - December 1953

10. Middleton, W. E. K. and Mungall, A. G., "The Luminous Directional Reflectance of Snow," Optical Society of America. Journal, v. 42, p. 572-579, August 1952

Navy Electronics Laboratory
Report 1150

OPTICAL PROPERTIES OF THE BERING SEA NAVAL ENVIRONMENT, JANUARY - FEBRUARY 1960, by J. M. Hood, Jr. 41p., 18 December 1962.

UNCLASSIFIED

As part of a continuing research into the geo-optics of the polar naval environment, optical and meteorological data were collected during 1960 winter naval exercises in the Bering Sea. The data have been analyzed and interpreted, and can now be used for the prediction of conditions influencing visibility, photographic and photoelectric surveillance, and equipment and personnel operations.

1. Arctic regions - Meteorological factors
2. Arctic regions - Optical factors

I. Hood, J. M., Jr.

SF 003 02 03, Task 0533
(NEL N6-4)

This card is UNCLASSIFIED.

Navy Electronics Laboratory
Report 1150

OPTICAL PROPERTIES OF THE BERING SEA NAVAL ENVIRONMENT, JANUARY - FEBRUARY 1960, by J. M. Hood, Jr. 41p., 18 December 1962.

UNCLASSIFIED

As part of a continuing research into the geo-optics of the polar naval environment, optical and meteorological data were collected during 1960 winter naval exercises in the Bering Sea. The data have been analyzed and interpreted, and can now be used for the prediction of conditions influencing visibility, photographic and photoelectric surveillance, and equipment and personnel operations.

1. Arctic regions - Meteorological factors
2. Arctic regions - Optical factors

I. Hood, J. M., Jr.

SF 003 02 03, Task 0533
(NEL N6-4)

This card is UNCLASSIFIED.

Navy Electronics Laboratory
Report 1150

OPTICAL PROPERTIES OF THE BERING SEA NAVAL ENVIRONMENT, JANUARY - FEBRUARY 1960, by J. M. Hood, Jr. 41p., 18 December 1962.

UNCLASSIFIED

As part of a continuing research into the geo-optics of the polar naval environment, optical and meteorological data were collected during 1960 winter naval exercises in the Bering Sea. The data have been analyzed and interpreted, and can now be used for the prediction of conditions influencing visibility, photographic and photoelectric surveillance, and equipment and personnel operations.

1. Arctic regions - Meteorological factors
2. Arctic regions - Optical factors

I. Hood, J. M., Jr.

SF 003 02 03, Task 0533
(NEL N6-4)

This card is UNCLASSIFIED.

Navy Electronics Laboratory
Report 1150

OPTICAL PROPERTIES OF THE BERING SEA NAVAL ENVIRONMENT, JANUARY - FEBRUARY 1960, by J. M. Hood, Jr. 41p., 18 December 1962.

UNCLASSIFIED

As part of a continuing research into the geo-optics of the polar naval environment, optical and meteorological data were collected during 1960 winter naval exercises in the Bering Sea. The data have been analyzed and interpreted, and can now be used for the prediction of conditions influencing visibility, photographic and photoelectric surveillance, and equipment and personnel operations.

1. Arctic regions - Meteorological factors
2. Arctic regions - Optical factors

I. Hood, J. M., Jr.

SF 003 02 03, Task 0533
(NEL N6-4)

This card is UNCLASSIFIED.

Initial Distribution List

Chief, Bureau of Ships
  Code 320 Code 360 Code 335
Chief, Bureau of Naval Weapons
  DLI-31 DLI-3 R-56
Chief of Naval Personnel, Library
Chief of Naval Operations
  OP-03EG OP-07T OP-76
Commander in Chief, PacFlt
Commander in Chief, LantFlt
Commander, Operational Test & Evaluation
  Force
Deputy Commander, Operational Test &
  Evaluation Force, Pac
Commander Training Command, PacFlt
Naval Air Development Center, Library
Naval Missile Center
  Library Code N3232
Naval Ordnance Laboratory, Library
Naval Ordnance Test Station, Pasadena
Naval Ordnance Test Station, China Lake, Library
David Taylor Model Basin
Navy Mine Defense Laboratory, Library
Navy Underwater Sound Laboratory, Library
ASW Tactical School, Lant Flt
Naval Engineering Experiment Station, Library
Naval Research Laboratory, Code 2027
Underwater Sound Reference Laboratory, Library
Beach Jumper Unit TWO
ASW School, San Diego
Office of Naval Research, Pasadena
Naval Oceanographic Office, Library (2)
Naval Postgraduate School, Library (2)
Office of Naval Research, San Francisco
DOD Research and Engineering, Technical Library
Assistant Chief of Staff for Intelligence
  U.S. Army R&D Branch
Aberdeen Proving Ground, Library (2)
Army Electronic Proving Ground
Frankford Arsenal, SMUFA-1031/65-1
Picatinny Arsenal, Library
Army Armor Human Research Unit
Army Proving Ground Center, PGAPI
Federal Aviation Agency
NASA, Langley Research Center (3)
Air Weather Service, Scott AFB
Bureau of Commercial Fisheries, Honolulu
Tufts University
University of Miami
  Marine Laboratory Library (3)